

Chemical freeze-out temperature in hydrodynamical description of Au+Au collisions at $\sqrt{s_{\text{NN}}} = 200$ GeV

Pasi Huovinen^a

Department of Physics, University of Virginia, P.O. Box 400714, Charlottesville, VA 22904-4714, USA
 e-mail: ph4h@virginia.edu

February 9, 2022

Abstract. We study the effect of separate chemical and kinetic freeze-outs to the ideal hydrodynamical flow in Au+Au collisions at RHIC ($\sqrt{s_{\text{NN}}} = 200$ GeV energy). Unlike earlier studies we explore how these effects can be counteracted by changes in the initial state of the hydrodynamical evolution. We conclude that the reproduction of pion, proton and antiproton yields necessitates a chemical freeze-out temperature of $T \approx 150$ MeV instead of $T = 160\text{--}170$ MeV motivated by thermal models. Contrary to previous reports, this lower temperature makes it possible to reproduce the p_T -spectra of hadrons if one assumes very small initial time, $\tau_0 = 0.2$ fm/c. However, the p_T -differential elliptic flow, $v_2(p_T)$ remains badly reproduced. This points to the need to include dissipative effects (viscosity) or some other refinement to the model.

PACS. 25.75.Dw Particle and resonance production – 25.75.Ld Collective flow

1 Introduction

Ideal fluid hydrodynamical models have been very successful in describing the bulk behaviour of particles formed in heavy-ion collisions at RHIC. The low- p_T single particle spectra as well as the transverse momentum dependence of elliptic anisotropy ($v_2(p_T)$) are reproduced nicely [1, 2]. This success has been one of the reasons to conclude that partonic state of matter with exceptionally low shear viscosity has been formed at RHIC [3].

However, these results have been achieved using ideal fluid hydrodynamical models, which assumed chemical equilibrium until the very end of the evolution of the system. This assumption is questionable, since the cross-sections of inelastic, particle number changing processes, are smaller than the cross-sections of elastic and quasi-elastic processes. Thus it is natural to assume that the system would still maintain local kinetic equilibrium when it begins to deviate from local chemical equilibrium.

This kind of approach is also supported by experimental data. The final hadron abundances in Au+Au collisions at RHIC can be well described by a hadron gas in approximate chemical equilibrium at $T_{\text{ch}} \approx 160\text{--}175$ MeV [4, 5]. The reproduction of the slopes of particle distributions using a blast-wave model requires much lower temperatures around $T_{\text{kin}} \approx 90\text{--}130$ MeV (depending on centrality) [6]. The hydrodynamical models assuming chemical equilibrium usually require freeze-out temperatures close to the

blast-wave fits¹ and cannot reproduce all observed particle yields simultaneously. It is thus reasonable to postulate two separate freeze-outs: first a chemical freeze-out where the yields of various particle species are fixed (frozen out) and somewhat later a kinetic freeze-out where the particles scatter for the last time and the momentum distributions cease to evolve.

The formalism to describe such a chemically frozen hadron gas has been known for quite a long time [9]. There have been several applications of this formalism to the hydrodynamical description of heavy ion collisions at SPS ($\sqrt{s_{\text{AA}}} = 17$ GeV) and RHIC ($\sqrt{s_{\text{AA}}} = 130$ and 200 GeV) energies [10, 11, 12, 13], but the results have been unsatisfactory. The conclusion of these studies has been that if the chemical composition of the hadron gas freezes out at hadronization, an ideal fluid hydrodynamical model can reproduce neither the single particle spectra nor the p_T -differential anisotropy [14, 15]. However, these studies are lacking in such a sense that they used the same initial state for both the chemically equilibrated and chemically frozen description. It is known that p_T -distributions are sensitive not only to the equation of state and kinetic freeze-out temperature, but also to the initial pressure gradients, *i.e.* to the initial density distribution [16]. Here we redo the hydrodynamic calculations once more to explore whether there is such an initial state which leads to an acceptable reproduction of the p_T -spectra and elliptic flow of pions and antiprotons.

^a *Present address:* Department of Physics, Purdue University, West Lafayette, IN 47907, USA

¹ With the notable exception of refs. [7, 8].

2 Equation of State

As a baseline, we use an equation of state (EoS) in chemical equilibrium. We construct it in the usual way: The hadronic phase is described by ideal resonance gas consisting of all hadrons and resonances listed in the Particle Data Book [17] with mass below 2 GeV. The plasma phase is described by an ideal massless parton gas consisting of gluons and three quark flavours. There is a first order phase transition between these two phases at $T_c = 170$ MeV. Note that this EoS is slightly different from the EoS with a first order phase transition used in ref. [18] and EoS Q used in ref. [19]. The phase transition temperature in this work is $T_c = 170$ MeV instead of 165 MeV and the number of quark flavours in the plasma phase is 3 instead of 2.5. The latter results in slightly larger latent heat. As can be seen by comparing the results here and in ref. [18], these differences have only a small effect on the particle spectra and anisotropies. In the following we refer to this EoS and the corresponding initial state as CE.

We construct an EoS out of chemical equilibrium in the way outlined in ref. [9] and later applied in refs. [11, 12, 13]. Below the chemical freeze-out temperature all inelastic, particle number changing processes have ceased, but elastic and quasielastic scatterings are still frequent enough to keep the system in kinetic equilibrium. The quasielastic scatterings lead to frequent formation and decay of resonances, which means that the yields of resonances and their daughter particles, say ρ -mesons and pions, still are in relative chemical equilibrium. This approach is therefore called partial chemical equilibrium (PCE). The presence of resonances means that the actual particle number of any particle species is not conserved after chemical freeze-out, but the effective particle number is. The effective particle number is defined as $\bar{N}_i = N_i + \sum_j n_j^{(i)} N_j$, where N_i is the actual number of particle species i , $n_j^{(i)}$ is the number of particles i formed in the decay of resonance j including the branching ratios, and N_j is the number of resonances j . The sum is over all the resonances with lifetimes smaller than the characteristic lifetime of the system. We take the characteristic lifetime to be 10 fm/c irrespective of the actual lifetime of the system. The following particles and resonances have lifetimes longer than 10 fm/c and are thus considered stable:

$$\pi, K, \eta, \omega, p, n, \eta', \phi, \Lambda, \Sigma, \Xi, \Lambda(1520), \Xi(1530), \Omega,$$

and the corresponding antiparticles. The corresponding effective potential of resonances is obtained in a similar fashion: $\mu_j = \sum_i n_j^{(i)} \mu_i$, where the sum is over all decay products of the resonance j .

We treat each isospin state of each particle species independently. This results in 35 conserved quantities and chemical potentials in the chemically frozen stage. Tabulating the EoS as a function of 36 quantities (35 chemical potentials and temperature) is unpractical, but avoidable by taking the advantage of the isentropic nature of ideal fluid hydrodynamics. Since entropy is conserved, the ratio of the effective particle number density ($\bar{n}_i = \bar{N}_i/V$)

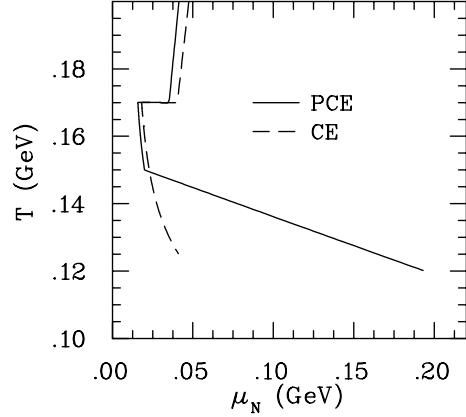


Fig. 1. Isentropic thermodynamic trajectories below 200 MeV at RHIC. PCE corresponds to chemically frozen calculation and CE corresponds to the center of the system in chemically equilibrated calculation. Above the phase transition temperature nucleon chemical potential $\mu_N = 3\mu_q$. The curves terminate at the kinetic freeze-out temperature ($\langle T_{\text{kin}} \rangle = 120$ and 125 MeV). Note that the difference above the chemical freeze-out temperature $T_{\text{ch}} = 150$ MeV is due to different initial states, see sect. 3. For PCE and CE, $s/n_B = 453.5$ and 395, respectively, where n_B is net baryon density.

and entropy density, \bar{n}_i/s , stays constant on streamlines of the flow. The expansion thus traces a trajectory of constant \bar{n}_i/s in $(T, \{\mu_i\})$ space and we need to evaluate the EoS only on this trajectory. The trajectories in the (T, μ_N) plane of the chemically frozen (PCE) and equilibrated systems (CE) at RHIC are shown in Fig. 1.

Qualitatively our EoS is similar to the EoSs in refs. [11, 12, 13]. The relation between pressure and energy density is almost identical in chemically equilibrated and frozen cases whereas at fixed energy density the chemically frozen system is much colder than a system in chemical equilibrium.

3 Initial conditions

We use the same boost-invariant hydrodynamic code as in ref. [18]. In the case of chemical equilibrium (CE) we use the same initial conditions as in ref. [18] for the equa-

Table 1. Initial time, phase transition temperature, chemical freeze-out temperature, kinetic freeze-out energy density and the corresponding average temperature on kinetic freeze-out surface used in chemical equilibrium (CE) and partial chemical equilibrium (PCE) calculations.

	CE	PCE
τ_0 (fm/c)	0.6	0.2
T_c (MeV)	170	170
T_{ch} (MeV)	—	150
ϵ_{kin} (GeV/fm ³)	0.065	0.117
$\langle T_{\text{kin}} \rangle$ (MeV)	125	120

Table 2. Measured and calculated particle yields at midrapidity in most central (0–5%) Au+Au collisions at $\sqrt{s_{\text{NN}}} = 200$ GeV. CE stands for chemical equilibrium, $T_{\text{ch}} = 170$ and 150 MeV denote cases where chemical freeze-out takes places at 170 and 150 MeV temperatures, respectively, but the initial state of the system is similar to the case CE. PCE is the final partial chemical equilibrium result where chemical freeze-out takes place at $T_{\text{ch}} = 150$ MeV and the initial conditions are adjusted to reproduce the observed p_T -distributions.

dN/dy	π^+	π^-	K^+	K^-	p	\bar{p}
PHENIX [31]	286.4 ± 24.2	281.8 ± 22.8	48.9 ± 5.2	45.7 ± 5.2	18.4 ± 2.6	13.5 ± 1.8
CE	273	273	44	42	10	5
$T_{\text{ch}} = 170$ MeV	268	268	52	50	25	20
$T_{\text{ch}} = 150$ MeV	265	265	51	49	18	13
PCE	278	278	53	51	18	14

tion of state with a first order phase transition: The initial entropy density distribution is a linear combination of the density of participants and binary collisions in the transverse plane whereas the initial baryon density is proportional to the number of participants. The parameter values are fixed to reproduce the p_T -spectra of pions and net protons ($p - \bar{p}$) in the most central collisions and the centrality dependence of charged hadron multiplicity at midrapidity. The initial time, phase transition temperature and freeze-out criteria for cases CE and PCE are shown in table 1. Note that the freeze-out energy density is slightly lower than in the corresponding calculation of ref. [18] because the EoS is slightly different (see sect. 2).

We find that the same initialization will not work in the chemically frozen case. To reproduce the slopes of the p_T -distributions we increase transverse flow by making the initial pressure gradients steeper and by starting the hydrodynamical evolution earlier. An acceptable result is achieved when the initial entropy density distribution is assumed to be proportional to the number of binary collisions in the transverse plane and the initial time is taken to be $\tau_0 = 0.2$ fm/ c .

This choice of initial time is bold since it requires hydrodynamics to be applicable almost immediately after the formation time of the partons of the system, but is nevertheless plausible [1,8]. First, in the pQCD+saturation method for calculating the particle production of ref. [8], the average energy and particle number densities are almost equal to those of a system of fixed temperature. Thus there is no need for particle number changing processes to achieve thermalization. Second, for massless particles, the relation between pressure and energy density is $\epsilon = 3P$ for any isotropic momentum distribution. Thus the use of hydrodynamics to describe the build-up of collective flow could be a reasonable assumption even if the momentum distribution differs from thermal equilibrium distribution. Third, this ideal gas EoS may be applicable very rapidly, since isotropization of the momentum distribution occurs much faster than thermal equilibration [20,21]. Finally, the studies of plasma instabilities support the notion of fast thermalization of the system [22].

If the proportionality between the initial entropy density and the number of binary collisions is independent of the centrality of the collision, the centrality dependence of the final particle multiplicity is not reproduced [23].

To correct this, we modify the parametrization given in ref. [23] by assuming an impact parameter dependent proportionality constant:

$$K_s(\tau_0 = 0.2 \text{ fm}; b) = 0.26942 \text{ fm}^{-6} b^3 + 10.9 \text{ fm}^{-4} b + 453.5 \text{ fm}^{-3},$$

and parametrize the initial entropy density in the transverse plane as

$$s(\mathbf{s}; \tau_0; \mathbf{b}) = K_s(\tau_0; b) T_A(\mathbf{s} + \frac{1}{2}\mathbf{b}) T_B(\mathbf{s} - \frac{1}{2}\mathbf{b}),$$

where T_A is the customary nuclear thickness function [23]. The initial baryon number distribution is obtained in the same way, *i.e.* it is taken to be proportional to the initial entropy density.

4 Particle yields and chemical freeze-out temperature

When separate chemical and kinetic freeze-outs are discussed in recent literature, chemical freeze-out is assumed to take place immediately after hadronization at $T_{\text{ch}} = 160\text{--}170$ MeV [10,11,12,13]. Either the ratios of all particle species are taken to be fixed at this temperature [11,12,13] or only strange particle yields are supposed to freeze-out [10]. The idea of chemical freeze-out at hadronization is conceptually attractive [24,25] and to some extent supported by thermal models which lead to temperatures [4,5] quite similar to the predicted phase transition temperature [26]. However, in the context of hydrodynamical model, we have found that assuming chemical freeze-out of all particle species at $T \approx 170$ MeV, leads to proton and antiproton yields that are too large when the model is tuned to reproduce the observed pion multiplicity. In most central collisions we obtain $dN_p/dy = 25$ protons and $dN_{\bar{p}}/dy = 20$ antiprotons at midrapidity instead of the experimentally observed yields of $dN_p/dy = 18.4 \pm 2.6$ and $dN_{\bar{p}}/dy = 13.5 \pm 1.8$ (see Table 2 and fig. 2, case $T_{\text{ch}} = 170$ MeV). This discrepancy is not surprising. Some thermal model fits to RHIC data have actually led to temperatures near or below 160 MeV rather than 170 MeV [27,28]. Thermal models also tend to lead to p/π ratios which are slightly larger than the experimental ratio, although still within experimental errors [27,28,29,30]. If the model

is required to fit only K/π and p/π ratios, the temperature is lower, $T \approx 152$ MeV [30].

As was argued in [15], the evolution of the average transverse momentum per particle, and thus the observed p_T spectra, is sensitive to pion number changing processes. In a hydrodynamical model it is thus important to describe the pion chemistry correctly and get the pion chemical freeze-out temperature right even if that means a worse reproduction of strange baryon yields. Inspired by the results of ref. [27], we take $T = 150$ MeV as the temperature where the pion number changing processes become negligible and the effective pion number freezes out. We expect that the better reproduction of the pion to proton and the pion to antiproton ratios gives a more realistic description of the temperature evolution and therefore of the evolution of particle distributions. As can be seen in the case $T_{\text{ch}} = 150$ MeV of Table 2, this approach gives the expected results: pion, kaon, proton and antiproton yields are almost exactly reproduced. The strange baryon yields, on the other hand, become too small at $T_{\text{ch}} = 150$ MeV.

The possible contribution from weak decays of strange particles causes a significant uncertainty in determining the chemical freeze-out temperature [4]. According to the PHENIX collaboration [31,32], the data has been corrected for the feed-down from weak decays of Λ 's and Σ^0 's, but whether the pion spectrum contains a contribution from K_S^0 decays, is not clearly explained. In these calculations we have assumed that there is no contribution from any weak decays in the PHENIX data. The decay of thermally produced K_S^0 's and Σ^\pm 's would increase the pion yield at midrapidity by ~ 40 pions and one proton/antiproton. For the cases $T_{\text{ch}} = 170$ and 150 MeV, the pion yield is thus at the experimental upper limit. The reduction of initial entropy by 5-10% would bring the pion yield closer to the experimental value and reduce the proton/antiproton yield by the same 5-10%. The proton and antiproton yields at $T_{\text{ch}} = 170$ MeV temperature would be too large in this case too. At $T_{\text{ch}} = 150$ MeV, the proton and antiproton yields would be within experimental errors, but one can argue that slightly larger freeze-out temperature $T_{\text{ch}} \approx 155$ MeV is favoured by the data.

In the case PCE the same procedure leads to pion yield larger than the data, which necessitates a larger adjustment in the initial entropy. However, after the adjustment, the conclusion is the same than for the cases $T_{\text{ch}} = 170$ and 150 MeV: Even if the pion yield contains a contribution from K_S^0 decays, $T_{\text{ch}} = 170$ MeV chemical freeze-out temperature leads to too large proton and antiproton yields and a temperature around $T_{\text{ch}} = 150$ – 155 MeV is favoured.

On the other hand, if the experimental correction for weak decays is not perfect and the spectra contains feed-down from strange baryons, the relative increase in the proton/antiproton yields would be larger than in the pion yield. In such a case the favoured freeze-out temperature would be even smaller than what is suggested here.

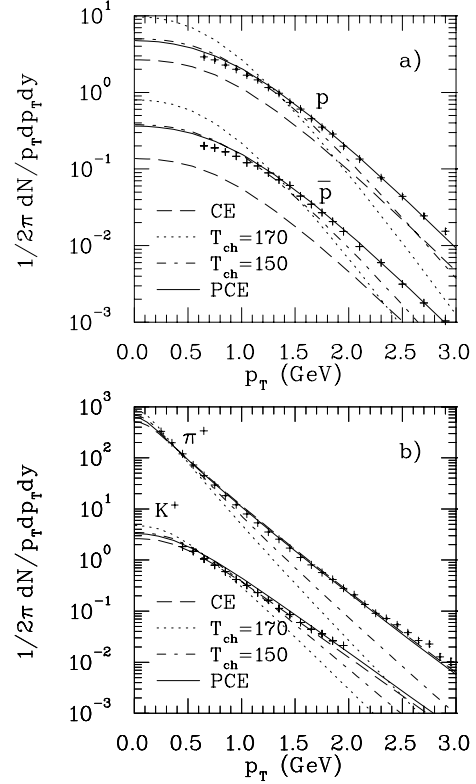


Fig. 2. (a) Proton and antiproton and (b) pion (π^+) and kaon (K^+) p_T -spectra in most central (0–5%) Au+Au collisions at $\sqrt{s_{\text{NN}}} = 200$ GeV compared with hydrodynamical calculations using different chemical freeze-out descriptions (see the text). The data was taken by the PHENIX collaboration [31]. For clarity the antiproton and kaon spectra are scaled by a factor 10^{-1} .

5 Transverse momentum spectra

The transverse momentum distributions for protons, antiprotons, pions and kaons in the most central collisions are shown in fig. 2. As before [18], the calculation with chemical equilibrium (CE) reproduces the pion and kaon data well, but it reproduces only the slopes of proton and antiproton distributions. If we proceed as in refs. [12, 13] and replace the EoS by an EoS with partial chemical equilibrium below $T_{\text{ch}} = 170$ MeV, adjust only the kinetic freeze-out density,² and keep everything else unchanged, the result is a disaster ($T_{\text{ch}} = 170$ in the figure). Even at $\langle T_{\text{kin}} \rangle = 100$ MeV average freeze-out temperature, the slopes of proton and antiproton spectra are far too steep. Decreasing the freeze-out temperature/density does not help the overall fit, since the pion spectrum becomes steeper with decreasing freeze-out temperature. This slightly counterintuitive behaviour was explained in ref. [15]. In boost-invariant expansion, transverse energy per unit rapidity, dE_T/dy , decreases with increasing time. In partial chemical equilibrium particle number is conserved and

² Note that in the actual calculation we use constant energy density as freeze-out criterion for numerical simplicity. In the following we talk about freeze-out temperature instead.

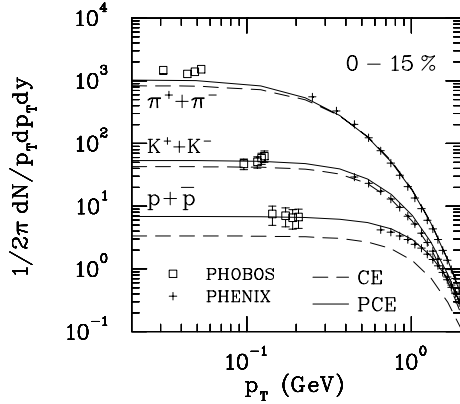


Fig. 3. Transverse momentum spectra of charged pions, charged kaons and protons + antiprotons in 15% most central Au+Au collisions at $\sqrt{s_{NN}} = 200$ GeV in the ultralow- p_T region measured by PHOBOS [33] compared with hydrodynamical calculations. The systematic and statistical errors of the PHOBOS data have been added in quadrature. The PHENIX data [31] are an average of the data in 0-5%, 5-10% and 10-15% centrality bins and have only statistical errors.

transverse energy has to be distributed among the same number of particles. Consequently $\langle p_T \rangle$ decreases and the slope of the p_T distribution steepens.

Another problem with $T_{ch} = 170$ MeV temperature can also be seen in fig. 2: There are too many protons and antiprotons as discussed in the previous section. This can be cured by decreasing the chemical freeze-out temperature to $T_{ch} = 150$ MeV. The calculation labelled $T_{ch} = 150$ in fig. 2 is performed in the same way as $T_{ch} = 170$. Only the EoS is changed, but the initial state is kept the same. When the kinetic freeze-out temperature is kept the same, $\langle T_{kin} \rangle = 100$ MeV, as for $T_{ch} = 170$, the particle distributions are closer to the data, but the slopes are still too steep. The flattening of the spectra is easy to understand. Between $T = 170$ and 150 MeV particle number is not conserved but the energy stored in masses of heavy particles is converted to kinetic energy of light particles (mostly pions) when the system cools. Thus $\langle p_T \rangle$ may increase even if dE_T/dy decreases, and $\langle p_T \rangle$ is larger at the time of chemical freeze-out when the particle number is fixed and pion $\langle p_T \rangle$ begins its slow decrease.

Neither the steeper initial profile given by the pure binary collision profile nor the small initial time $\tau_0 = 0.2$ fm/c is sufficient alone to create large enough flow before chemical freeze-out to fit the data. When these two are used together (PCE), the fit to the data is good. The fit to pion data is even better than in the chemical equilibrium case (CE) at low p_T , where PCE depicts a concave curvature typical for a finite pion chemical potential [34]. At low p_T the calculation still suffers from excess of protons and especially antiprotons as if even a larger flow velocity and a smaller chemical freeze-out temperature were necessary. We have checked that the binary collision profile and short initial time combined with an EoS with $T_{ch} = 170$ MeV does not lead to satisfactory reproduction of the slopes either, but the extra push created in the hadronic equilib-

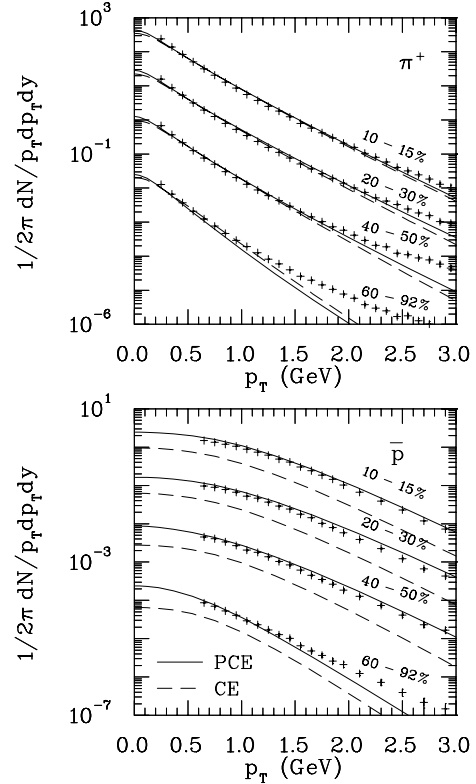


Fig. 4. Pion (π^+) and antiproton (\bar{p}) p_T -spectra in semi-central to peripheral Au+Au collisions at $\sqrt{s_{AA}} = 200$ GeV compared with hydrodynamical calculations (see text). The data was taken by the PHENIX collaboration [31]. For clarity the spectra at centralities 20 - 30%, 40 - 60% and 60 - 80% are scaled by factors 10^{-1} , 10^{-2} and 10^{-3} , respectively.

rium stage between $T = 170$ and 150 MeV temperatures is necessary to fit the data.

Figure 3 shows the results for the very low transverse momentum measured by the PHOBOS collaboration [33] as well as the spectra measured by the PHENIX collaboration [31] at larger p_T . The model PCE works well also at this p_T region reproducing the flat behaviour of the data. The spectrum of pions is slightly below the data. This was seen already in table 2 where pion multiplicity was shown to be slightly below the data but still within the experimental error. The increase in the initial entropy of the system to increase pion multiplicity would, however, necessitate even lower chemical freeze-out temperature not to exceed the observed kaon multiplicity.

Pion and antiproton p_T -spectra at various centralities are shown in fig. 4. The pattern is familiar from earlier hydrodynamical studies: The more peripheral the collisions, the narrower the p_T range where hydrodynamics can reproduce the spectra. An interesting detail is that antiproton spectra in semi-central collisions (20-30% and 40-50% of total cross section) is slightly too flat. As mentioned in the introduction, blast wave fits give higher kinetic freeze-out temperatures in peripheral than in central collisions. Hydrodynamical models have traditionally used fixed freeze-out temperature/density for simplicity,

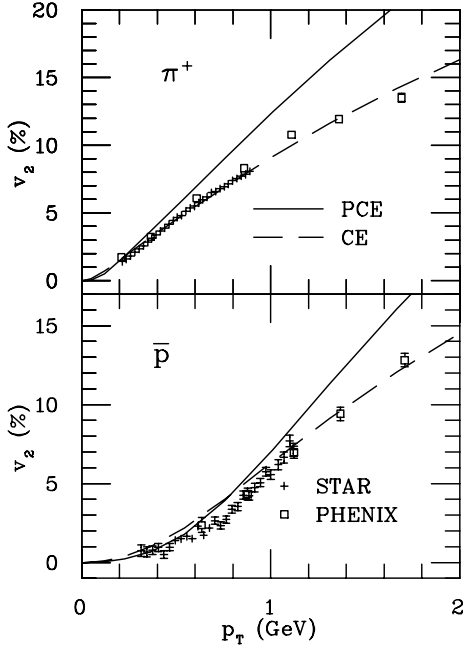


Fig. 5. Elliptic anisotropy of pions and antiprotons vs. transverse momentum in minimum bias Au+Au collisions at $\sqrt{s_{NN}} = 200$ GeV calculated using different chemical freeze-out descriptions (see text) and compared with the data by the STAR [35] and PHENIX [36] collaborations.

but the overshooting of antiproton spectra here suggests that a slightly larger kinetic freeze-out density in semi-central than in central collisions might lead to better results.

6 Elliptic anisotropy

Unfortunately the success in the previous section cannot be repeated for elliptic anisotropy. Figure 6 shows the p_T -differential elliptic anisotropy of pions and antiprotons in minimum bias Au+Au collisions. The trend is similar to that in ref. [12]. The chemical equilibrium result (CE) reproduces the pion data excellently and is slightly above the proton data. Partial chemical equilibrium (PCE) leads to a slope of the pion anisotropy that is too large and the calculated result is clearly above the data. The proton anisotropy is reproduced at $p_T < 600$ MeV, but increases too fast at larger momenta.

It is worth noticing that the different p_T -differential v_2 is mostly due to the different description of the hadron gas. As shown in ref. [12], the same initial state leads to different v_2 in chemically equilibrated and frozen cases. The basic reason for this is in the different temperature evolution in the hadron gas. When both systems have reached the same density, the collective flow field and its anisotropies are almost identical in both cases. However, the chemically equilibrated system is hotter and thus the random thermal motion is stronger. Thermal motion smears away the underlying anisotropy of the collective flow field, and,

therefore, the final v_2 of particles of the chemically equilibrated system is smaller than the v_2 of particles of the corresponding chemically frozen system³.

Comparison of these results with the recent results obtained using viscous hydrodynamics [37,38,39] is particularly interesting. Dissipation reduces elliptic flow and it was claimed in ref. [39] that even the postulated minimal shear viscosity $\frac{\eta}{s} = \frac{1}{4\pi}$ causes very large suppression. As shown here, suppression of elliptic flow is required to fit the data when chemical equilibrium is lost in the hadron gas. However, the actual size of the allowed viscous correction is unknown since the EoS affects especially the proton anisotropy. At least in the chemically equilibrated case, the lattice QCD based EoS leads to even larger proton $v_2(p_T)$ than the EoS used here [18]. Whether finite shear viscosity leads to a correct reproduction of the data remains to be seen as well as how large of a viscosity is allowed in plasma and hadronic phases [40].

7 Summary and discussion

Contrary to previous reports [12,13,14,15], we have shown that it is possible to reproduce both (nonstrange) hadron yields and their transverse momentum spectra using ideal fluid hydrodynamics with separate chemical and kinetic freeze-outs. The difference between our approach and the previous studies is that we used a different initial state for the chemically frozen system than for the system in chemical equilibrium, adjusted the initial time to be as small as $\tau_0 = 0.2$ fm/c and changed the chemical freeze-out temperature to be below the phase transition temperature to $T_{ch} = 150$ MeV. However, our success is incomplete. Even after these adjustments of the model, we were not able to reproduce the p_T -differential elliptic flow of pions and protons. To describe particle yields, their p_T -distributions and anisotropies, the description of expansion has to be amended, most probably by including dissipative effects: viscosity and diffusion.

Nevertheless, our results demonstrate how sensitive the expansion dynamics during the hadronic phase is to hadron chemistry. Good knowledge of hadron chemistry is therefore essential if we wish to extract the viscosity of the QGP from the experimental data using viscous hydrodynamics. The recent method of choice for this purpose has been the so called hybrid hydro+cascade model where the expansion is described using hydrodynamics until the system is hadronized and the hadronic phase is described using hadronic cascade [40,41,42,43]. These models have the advantage that the dissipative effects and hadronic chemistry are included in the model and the kinetic freeze-out is a result of hadronic cross sections without any free parameters. So far cascade models used in these hybrid models have been limited to two particle scatterings, but it has been argued that multiparticle processes are essential for reproducing the proton and antiproton yields [44, 45]. It is therefore not surprising that hydro+cascade models may have difficulties in reproducing antiproton spec-

³ For a more detailed discussion see ref. [15].

trum at the lowest values of transverse momentum [43]. On the other hand, multiparticle processes are included in hydrodynamical models and as argued in sect. 5, processes where heavy particles annihilate and form lighter particles, and vice versa, are important for the build-up of flow. For this reason we consider that a hydrodynamical description of the hadronic phase is still worth pursuing as a complementary tool to hybrid models, even if there are transport models where the multiparticle processes are included [45].

Another conclusion of these results is that the final spectra are sensitive to the details of the initial state. As already stated in ref. [40], theoretical constraints to the initial state and especially to its shape are of utmost importance if we wish to extract the properties of the QGP from experimental data.

Some arguments favouring the use of hydrodynamics already at initial time $\tau_0 = 0.2$ fm/c were given in sect. 3. We admit that in a certain sense our result is similar to ref. [13], where Kolb and Rapp claimed that it is not possible to fit the p_T -spectra without pre-hydrodynamic transverse flow. Some of our arguments favouring the use of hydrodynamics at $\tau = 0.2$ fm/c centered on the fact that for the relation $\epsilon = 3P$ to hold, it is sufficient that the momentum distribution is isotropic. It does not need to be thermal. Thus one may say that we are using hydrodynamics to calculate the pre-hydrodynamic transverse flow, although the flow field in our case is different from the one used in ref. [13].

The low chemical freeze-out temperature $T_{\text{ch}} = 150$ MeV clearly below the phase transition temperature $T_c = 170$ MeV leads to another problem. The chemical freeze-out temperature is almost independent of centrality [30]. It was argued in ref. [25] that such an independence requires either chemical freeze-out at phase transition or extremely steep temperature dependence of the inelastic scattering rate. One way to solve this apparent discrepancy is to assume that the chemical equilibration in the hadron gas close to T_c is very fast indeed due to massive Hagedorn resonances [46]. These resonances couple to multi-pion states and baryon-antibaryon pairs and thus lead to fast chemical equilibration, but they appear only close to the critical temperature.

The treatment of hadronic chemistry and choice of chemical freeze-out used in this paper is by no means the final one. Since the data seem to favour the notion that strange baryon yields are fixed at higher temperature than the yields of pions, kaons and nucleons/antinucleons, it would be relatively easy to use two separate chemical freeze-out temperatures: one for strange baryons and another for everything else. Another relatively straightforward improvement is to redo the calculation of the chemical relaxation rate of pions [47] for the RHIC environment and to use it to dynamically find the local chemical freeze-out temperature by comparing this rate to the expansion rate. This approach is particularly appealing if the kinetic freeze-out surface is also found by comparing the scattering and expansion rates. Finally, it would be useful to calculate the particle yields dynamically during the

evolution using actual rate equations for particle number changing processes. For baryons, preliminary study was already done in ref. [48], but in that work mesons were supposed to be in chemical equilibrium and the EoS was independent of baryon and antibaryon densities. A proper calculation would require dynamical treatment of mesons and calculating the EoS using actual particle densities.

I thank K. Haglin, T. Hirano, H. Honkanen, S. Pratt, P.V. Ruuskanen, S.S. Räsänen and G. Torrieri for many enlightening discussions. Financial support from Johannes Rättendahl foundation is also gratefully acknowledged.

References

1. P. Huovinen and P. V. Ruuskanen, *Ann. Rev. Nucl. Part. Sci.* **56** (2006) 163 [arXiv:nucl-th/0605008].
2. P. F. Kolb and U. W. Heinz, in *Quark-Gluon Plasma 3*, eds. R. C. Hwa and X. N. Wang (World Scientific, Singapore, 2004), p. 634 [arXiv:nucl-th/0305084].
3. M. Gyulassy and L. McLerran, *Nucl. Phys. A* **750** (2005) 30 [arXiv:nucl-th/0405013].
4. P. Braun-Munzinger, K. Redlich and J. Stachel, in *Quark-Gluon Plasma 3*, eds. R. C. Hwa and X. N. Wang (World Scientific, Singapore, 2004), p. 491 [arXiv:nucl-th/0304013].
5. J. Adams *et al.* [STAR Collaboration], *Nucl. Phys. A* **757** (2005) 102 [arXiv:nucl-ex/0501009].
6. J. Adams *et al.* [STAR Collaboration], *Phys. Rev. Lett.* **92** (2004) 112301 [arXiv:nucl-ex/0310004].
7. K. J. Eskola, H. Niemi, P. V. Ruuskanen and S. S. Rasanen, *Phys. Lett. B* **566** (2003) 187 [arXiv:hep-ph/0206230].
8. K. J. Eskola, H. Honkanen, H. Niemi, P. V. Ruuskanen and S. S. Rasanen, *Phys. Rev. C* **72** (2005) 044904 [arXiv:hep-ph/0506049].
9. H. Bebie, P. Gerber, J. L. Goity and H. Leutwyler, *Nucl. Phys. B* **378**, (1992) 95.
10. N. Arbex, F. Grassi, Y. Hama and O. Socolowski, *Phys. Rev. C* **64**, (2001) 064906; W. L. Qian, R. Andrade, F. Grassi, O. J. Socolowski, T. Kodama and Y. Hama, *Int. J. Mod. Phys. E* **16** (2007) 1877 [arXiv:nucl-th/0703078]; W. L. Qian, R. Andrade, F. Grassi, Y. Hama and T. Kodama, arXiv:0709.0845 [nucl-th].
11. D. Teaney, arXiv:nucl-th/0204023.
12. T. Hirano and K. Tsuda, *Phys. Rev. C* **66**, (2002) 054905 [arXiv:nucl-th/0205043].
13. P. F. Kolb and R. Rapp, *Phys. Rev. C* **67**, (2003) 044903 [arXiv:hep-ph/0210222].
14. K. Adcox *et al.* [PHENIX Collaboration], *Nucl. Phys. A* **757** (2005) 184 [arXiv:nucl-ex/0410003].
15. T. Hirano and M. Gyulassy, *Nucl. Phys. A* **769** (2006) 71 [arXiv:nucl-th/0506049].
16. A. Dumitru and D. H. Rischke, *Phys. Rev. C* **59**, (1999) 354 [arXiv:nucl-th/9806003].
17. S. Eidelman *et al.* [Particle Data Group], *Phys. Lett. B* **592** (2004) 1.
18. P. Huovinen, *Nucl. Phys. A* **761**, (2005) 296 [arXiv:nucl-th/0505036].
19. P. F. Kolb, J. Sollfrank and U. W. Heinz, *Phys. Rev. C* **62**, (2000) 054909 [arXiv:hep-ph/0006129].

20. J. Berges, S. Borsanyi and C. Wetterich, Nucl. Phys. B **727**, (2005) 244 [arXiv:hep-ph/0505182].
21. Y. V. Kovchegov and A. Taliotis, Phys. Rev. C **76**, (2007) 014905 [arXiv:0705.1234 [hep-ph]].
22. S. Mrowczynski, Acta Phys. Polon. B **37** (2006) 427 [arXiv:hep-ph/0511052].
23. P. F. Kolb, U. W. Heinz, P. Huovinen, K. J. Eskola and K. Tuominen, Nucl. Phys. A **696**, (2001) 197 [arXiv:hep-ph/0103234].
24. B. Muller, arXiv:nucl-th/0508062.
25. U. Heinz and G. Kestin, PoS C **POD2006** (2006) 038 [arXiv:nucl-th/0612105].
26. F. Karsch and E. Laermann, in *Quark-Gluon Plasma 3*, eds. R. C. Hwa and X. N. Wang (World Scientific, Singapore, 2004), p. 1 [arXiv:hep-lat/0305025].
27. M. Kaneta and N. Xu, arXiv:nucl-th/0405068.
28. A. Andronic, P. Braun-Munzinger and J. Stachel, Nucl. Phys. A **772**, (2006) 167 [arXiv:nucl-th/0511071].
29. A. Baran, W. Broniowski and W. Florkowski, Acta Phys. Polon. B **35**, (2004) 779 [arXiv:nucl-th/0305075].
30. J. Cleymans, B. Kampfer, M. Kaneta, S. Wheaton and N. Xu, Phys. Rev. C **71**, (2005) 054901 [arXiv:hep-ph/0409071].
31. S. S. Adler *et al.* [PHENIX Collaboration], Phys. Rev. C **69**, (2004) 034909 [arXiv:nucl-ex/0307022].
32. Roy Lacey, private communication.
33. B. B. Back *et al.* [PHOBOS Collaboration], Phys. Rev. C **70**, (2004) 051901 [arXiv:nucl-ex/0401006].
34. M. Kataja and P. V. Ruuskanen, Phys. Lett. B **243** (1990) 181.
35. J. Adams *et al.* [STAR Collaboration], Phys. Rev. C **72**, (2005) 014904 [arXiv:nucl-ex/0409033].
36. S. S. Adler *et al.* [PHENIX Collaboration], Phys. Rev. Lett. **91**, (2003) 182301 [arXiv:nucl-ex/0305013].
37. A. K. Chaudhuri, arXiv:0704.0134 [nucl-th].
38. P. Romatschke and U. Romatschke, Phys. Rev. Lett. **99** (2007) 172301 [arXiv:0706.1522 [nucl-th]].
39. H. Song and U. W. Heinz, Phys. Lett. B **658** (2008) 279 [arXiv:0709.0742 [nucl-th]].
40. T. Hirano, U. W. Heinz, D. Kharzeev, R. Lacey and Y. Nara, Phys. Lett. B **636**, (2006) 299 [arXiv:nucl-th/0511046].
41. S. A. Bass and A. Dumitru, Phys. Rev. C **61** (2000) 064909 [arXiv:nucl-th/0001033].
42. D. Teaney, J. Lauret and E. V. Shuryak, arXiv:nucl-th/0110037.
43. C. Nonaka and S. A. Bass, Phys. Rev. C **75**, (2007) 014902 [arXiv:nucl-th/0607018].
44. R. Rapp and E. V. Shuryak, Phys. Rev. Lett. **86** (2001) 2980 [arXiv:hep-ph/0008326]; R. Rapp, Phys. Rev. C **66**, (2002) 017901 [arXiv:hep-ph/0204131].
45. W. Cassing, Nucl. Phys. A **700** (2002) 618 [arXiv:nucl-th/0105069].
46. J. Noronha-Hostler, C. Greiner and I. A. Shovkovy, arXiv:nucl-th/0703079.
47. S. Pratt and K. Haglin, Phys. Rev. C **59**, (1999) 3304.
48. P. Huovinen and J. I. Kapusta, Phys. Rev. C **69**, (2004) 014902 [arXiv:nucl-th/0310051].